

STUDY OF HEAT GENERATION EFFECTS ON MHD FLOW IN POROUS MEDIUM

In this chapter, mathematical modelling of heat generation/absorption and chemical reaction effects on unsteady Casson fluid flow in presence of magnetic field over an exponentially accelerated plate embedded in porous medium is considered. It is considered that bounding plate has ramped as well as isothermal boundary condition for temperature and concentration profiles. This phenomenon is modelled in the form of partial differential equations with initial boundary conditions. Expression for velocity, temperature and concentration profiles are obtained using Laplace transform technique from governing dimensionless equations. Exact expressions for shear stress, temperature gradient and concentration gradient are derived and presented in tabular form.

5.1 Introduction of the Problem

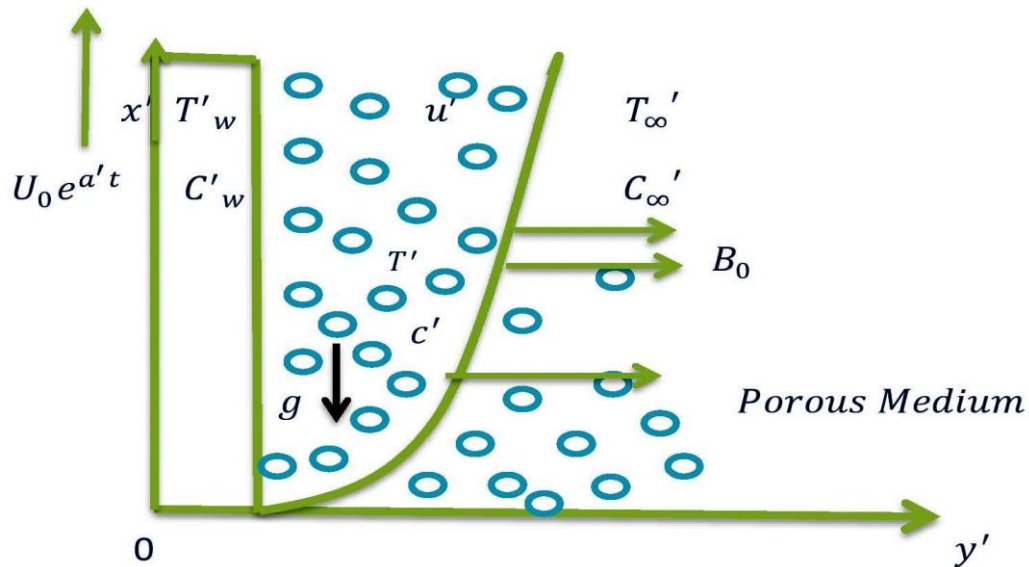
Heat generation/absorption effects have important role in the heat transfer characteristics of numerous physical difficulties of real-world interest viz. convection in Earth's mantle, heat removal, development of metal waste from spent nuclear fuel, cooling of electronic components, applications in the field of nuclear energy etc. Therefore, it is suitable to deliberate temperature dependent heat source and/or sink which may have strong impact on heat transfer characteristics of the fluid flow problems. Taking into consideration this fact, Sparrow and Cess [162] studied effect of temperature-dependent heat sources or sinks in a stagnation point flow. Relevant studies on this topic are also discussed in Kamel [163] and Chamkha [164]. Recently, Hayat et al. [114] considered MHD three-dimensional flow of Maxwell fluid with heat source/sink, whereas Shehzad et al. [115] discussed three-dimensional Casson fluid of MHD flow in porous medium with heat generation.

Combine effects of heat generation and chemical reaction on Casson fluid of MHD flow past an exponentially accelerated plate in porous medium is important in engineering and technology. Recently, Hussain et al. [135] considered free convective heat transfers with heat absorption and chemical reaction over an accelerated moving plate in a rotating system, whereas Seth et al. [148] studied MHD flow with radiation and heat absorption over an exponentially accelerated vertical plate with ramped temperature. Raju et al. [119] obtained analytical and numerical solution of unsteady MHD flow with heat absorption.

5.2 Novelty of the Problem

Aim of this chapter to extend earlier research work which discussed in Section-I of chapter 3 due to the effects of heat generation/absorption on MHD flow of Casson fluid past over an exponentially accelerated vertical plate embedded in porous medium with ramped boundary conditions. To obtain analytical results of governing linear partial differential equations, Laplace transform technique can be used. Such study may find applications in solar collection systems, fire dynamics in insulations, catalytic reactors, nuclear waste repositories, recovery of petroleum products and gases etc.

5.3 Mathematical Formulation of the Problem



$$T' = \begin{cases} T'_\infty + (T'_w - T'_\infty) t'/t_0 & \text{if } 0 < t' < t_0 \\ T'_w & \text{if } t' \geq t_0 \end{cases}, C' = \begin{cases} C'_\infty + (C'_w - C'_\infty) t'/t_0 & \text{if } 0 < t' < t_0 \\ C'_w & \text{if } t' \geq t_0 \end{cases}; y' = 0$$

Figure 5.1: Physical sketch of the Model.

In Figure 5.1, the flow is being kept to $y' > 0$, where y' is measured in the normal direction to the plate and x' - axis is along the wall. Initially, at $t' \leq 0$, fluid and plate are at rest, temperature T'_∞ and concentration to be C'_∞ . At time $t' > 0$, the temperature of the plate is either raised or lowered to $T'_\infty + (T'_w + T'_\infty) t'/t_0$ when $t' \leq t_0$ and T'_w when $t' > t_0$ respectively which is there after maintained constant T'_w and the level of concentration at the surface of the plate is raised or

lowered to $C'_\infty + (C'_w + C'_\infty) t'/t_0$ when $t' \leq t_0$ and C'_w when $t' > t_0$ respectively which is there after maintained constant C'_w . The uniform transverse magnetic field B_0 applied in parallel direction that of y' - axis. Under above assumptions and the Boussinesq's approximation, governing equations are given below:

$$\rho \frac{\partial u'}{\partial t'} = \mu\beta \left(1 + \frac{1}{\gamma}\right) \frac{\partial^2 u'}{\partial y'^2} - \sigma B_0^2 u' - \frac{\mu\phi}{k'} u' + \rho g \beta'_T (T' - T'_\infty) + \rho g \beta'_C (C' - C'_\infty) \quad (5.1)$$

$$\frac{\partial T'}{\partial t'} = \frac{k_4}{\rho c_p} \frac{\partial^2 T'}{\partial y'^2} + \frac{Q_0}{\rho c_p} (T' - T'_\infty) \quad (5.2)$$

$$\frac{\partial C'}{\partial t'} = D_M \frac{\partial^2 C'}{\partial y'^2} - k'_2 (C' - C'_\infty) \quad (5.3)$$

with following initial and boundary conditions

$$u' = 0, \quad T' = T'_\infty, \quad C' = C'_\infty; \text{ as } y' \geq 0 \text{ and } t' \leq 0$$

$$u' = U_0 e^{a't} \text{ as } t' > 0 \text{ and } y' = 0, \quad T' = \begin{cases} T'_\infty + (T'_w - T'_\infty) t'/t_0 & \text{if } 0 < t' < t_0, \\ T'_w & \text{if } t' \geq t_0 \end{cases},$$

$$C' = \begin{cases} C'_\infty + (C'_w - C'_\infty) t'/t_0 & \text{if } 0 < t' < t_0; \\ C'_w & \text{if } t' \geq t_0 \end{cases}; y' = 0$$

$$u' \rightarrow 0, T' \rightarrow T'_\infty, \quad C' \rightarrow C'_\infty; \text{ as } y' \rightarrow \infty \text{ and } t' \geq 0 \quad (5.4)$$

Introducing the following dimensionless quantities

$$y = \frac{y'}{U_0 t_0}, \quad u = \frac{u'}{U_0}, \quad t = \frac{t'}{t_0}, \quad \theta = \frac{(T' - T'_\infty)}{(T'_w - T'_\infty)}, \quad C = \frac{(C' - C'_\infty)}{(C'_w - C'_\infty)}, \quad Gr = \frac{\nu g \beta'_T (T'_w - T'_\infty)}{U_0^3}, \quad Gm = \frac{\nu g \beta'_C (C'_w - C'_\infty)}{U_0^3},$$

$$M = \frac{\sigma B_0^2 \nu}{\rho U_0^2}, \quad Pr = \frac{\rho c_p}{k_4}, \quad H = \frac{Q_0 \nu}{\rho c_p U_0^2}, \quad Sc = \frac{\nu}{D_M}, \quad Kr = \frac{\nu k'_2}{U_0^2}, \quad \gamma = \frac{\mu_B \sqrt{2\pi c}}{P_y}, \quad \tau = \frac{\tau}{\rho u^2}$$

In the equations (5.1) to (5.4) dropping out the " ' " notation (for simplicity),

$$\frac{\partial u}{\partial t} = \left(1 + \frac{1}{\gamma}\right) \frac{\partial^2 u}{\partial y^2} - \left(M^2 + \frac{1}{k}\right) u + G_r \theta + G_m C \quad (5.5)$$

$$\frac{\partial \theta}{\partial t} = \frac{1}{Pr} \frac{\partial^2 \theta}{\partial y^2} + H \theta \quad (5.6)$$

$$\frac{\partial C}{\partial t} = \frac{1}{Sc} \frac{\partial^2 C}{\partial y^2} - Kr C \quad (5.7)$$

with initial and boundary condition

$$u = \theta = C = 0 \text{ as } y \geq 0, t = 0$$

$$u = e^{a't}, \theta = \begin{cases} t, & 0 < t \leq 1 \\ 1 & t > 1 \end{cases}, C = \begin{cases} t, & 0 < t \leq 1 \\ 1 & t > 1 \end{cases} \text{ as } y = 0, t > 0$$

$$u \rightarrow 0, \theta \rightarrow 0, C \rightarrow 0 \text{ as } y \rightarrow \infty, t > 0 \quad (5.8)$$

5.4 Solution of the Problem

Expressions for velocity, temperature and concentration profiles are derived by solving equations (5.5) to (5.8) with the help of Laplace transform technique.

5.4.1 Solution of the problem for ramped temperature and ramped surface concentration

$$\theta(y, t) = f_6(y, t) - f_6(y, t - 1)H(t - 1) \quad (5.9)$$

$$C(y, t) = f_9(y, t) - f_9(y, t - 1)H(t - 1) \quad (5.10)$$

$$u(y, t) = g_1(y, t) + i_1(y, t) - i_1(y, t - 1)H(t - 1) \quad (5.11)$$

5.4.2 Solution of the problem for isothermal temperature and ramped surface concentration

In this case, the boundary conditions are the same excluding equations (5.8) that becomes $\theta = 1$ at $y = 0, t \geq 0$. So, expression for velocity and temperature profiles are obtained with isothermal temperature which is given below.

$$\theta(y, t) = f_5(y, t) \quad (5.12)$$

$$u(y, t) = g_1(y, t) + g_5(y, t) + g_6(y, t) - g_6(y, t - 1)H(t - 1) - g_7(y, t) - g_4(y, t) + g_4(y, t - 1)H(t - 1) \quad (5.13)$$

where

$$i_1(y, t) = g_2(y, t) - g_3(y, t) - g_4(y, t) \quad (5.14)$$

$$g_1(y, t) = \frac{e^{a't}}{2} \left[e^{-y\sqrt{\frac{1}{a}(b+a')}} \operatorname{erfc} \left(\frac{y}{2\sqrt{at}} - \sqrt{(b+a')t} \right) + e^{y\sqrt{\frac{1}{a}(b+a')}} \operatorname{erfc} \left(\frac{y}{2\sqrt{at}} + \sqrt{(b+a')t} \right) \right] \quad (5.15)$$

$$g_2(y, t) = a_{15}f_1(y, t) + a_{16}f_2(y, t) + a_{10}f_3(y, t) + a_{13}f_4(y, t) \quad (5.16)$$

$$g_3(y, t) = a_{11}f_5(y, t) + a_9f_6(y, t) + a_{10}f_7(y, t) \quad (5.17)$$

$$g_4(y, t) = a_{14}f_8(y, t) + a_{12}f_9(y, t) + a_{13}f_{10}(y, t) \quad (5.18)$$

$$g_5(y, t) = a_9f_1(y, t) - a_9f_3(y, t) \quad (5.19)$$

$$g_6(y, t) = a_{14}f_1(y, t) + a_{12}f_2(y, t) + a_{13}f_4(y, t) \quad (5.20)$$

$$g_7(y, s) = a_9f_5(y, t) - a_9f_7(y, t) \quad (5.21)$$

$$f_1(y, t) = \frac{1}{2} \left[e^{-y\sqrt{\frac{b}{a}}} \operatorname{erfc} \left(\frac{y}{2\sqrt{at}} - \sqrt{bt} \right) + e^{y\sqrt{\frac{b}{a}}} \operatorname{erfc} \left(\frac{y}{2\sqrt{at}} + \sqrt{bt} \right) \right] \quad (5.22)$$

$$f_2(y, t) = \frac{1}{2} \left[\left(t - \frac{y}{2\sqrt{ab}} \right) e^{-y\sqrt{\frac{b}{a}}} \operatorname{erfc} \left(\frac{y}{2\sqrt{at}} - \sqrt{bt} \right) + \left(t + \frac{y}{2\sqrt{ab}} \right) e^{y\sqrt{\frac{b}{a}}} \operatorname{erfc} \left(\frac{y}{2\sqrt{at}} + \sqrt{bt} \right) \right] \quad (5.23)$$

$$f_3(y, t) = \frac{e^{a_3t}}{2} \left[e^{-y\sqrt{\frac{1}{a}(b+a_3)}} \operatorname{erfc} \left(\frac{y}{2\sqrt{at}} - \sqrt{(b+a_3)t} \right) + e^{y\sqrt{\frac{1}{a}(b+a_3)}} \operatorname{erfc} \left(\frac{y}{2\sqrt{at}} + \sqrt{(b+a_3)t} \right) \right] \quad (5.24)$$

$$f_4(y, t) = \frac{e^{-a_7t}}{2} \left[e^{-y\sqrt{\frac{1}{a}(b-a_7)}} \operatorname{erfc} \left(\frac{y}{2\sqrt{at}} - \sqrt{(b-a_7)t} \right) + e^{y\sqrt{\frac{1}{a}(b-a_7)}} \operatorname{erfc} \left(\frac{y}{2\sqrt{at}} + \sqrt{(b-a_7)t} \right) \right] \quad (5.25)$$

$$f_5(y, t) = \frac{1}{2} \left[e^{-y\sqrt{(-H)Pr}} \operatorname{erfc} \left(\frac{y\sqrt{Pr}}{2\sqrt{t}} - \sqrt{(-H)t} \right) + e^{y\sqrt{(-H)Pr}} \operatorname{erfc} \left(\frac{y\sqrt{Pr}}{2\sqrt{t}} + \sqrt{(-H)t} \right) \right] \quad (5.26)$$

$$f_6(y, t) = \frac{1}{2} \left[\left(t - \frac{y\sqrt{Pr}}{2\sqrt{(-H)}} \right) e^{-y\sqrt{(-H)Pr}} \operatorname{erfc} \left(\frac{y\sqrt{Pr}}{2\sqrt{t}} - \sqrt{(-H)t} \right) + \left(t + \frac{y\sqrt{Pr}}{2\sqrt{(-H)}} \right) e^{y\sqrt{(-H)Pr}} \operatorname{erfc} \left(\frac{y\sqrt{Pr}}{2\sqrt{t}} + \sqrt{(-H)t} \right) \right] \quad (5.27)$$

$$f_7(y, t) = \frac{e^{a_3t}}{2} \left[e^{-y\sqrt{Pr(-H+a_3)}} \operatorname{erfc} \left(\frac{y\sqrt{Pr}}{2\sqrt{t}} - \sqrt{(-H+a_3)t} \right) + e^{y\sqrt{Pr(-H+a_3)}} \operatorname{erfc} \left(\frac{y\sqrt{Pr}}{2\sqrt{t}} + \sqrt{(-H+a_3)t} \right) \right] \quad (5.28)$$

$$f_8(y, t) = \frac{1}{2} \left[e^{-y\sqrt{KrSc}} \operatorname{erfc} \left(\frac{y\sqrt{Sc}}{2\sqrt{t}} - \sqrt{Kr t} \right) + e^{y\sqrt{KrSc}} \operatorname{erfc} \left(\frac{y\sqrt{Sc}}{2\sqrt{t}} + \sqrt{Kr t} \right) \right] \quad (5.29)$$

$$f_9(y, t) = \frac{1}{2} \left[\left(t - \frac{y\sqrt{Sc}}{2\sqrt{Kr}} \right) e^{-y\sqrt{ScKr}} \operatorname{erfc} \left(\frac{y\sqrt{Sc}}{2\sqrt{t}} - \sqrt{Kr t} \right) + \left(t + \frac{y\sqrt{Sc}}{2\sqrt{Kr}} \right) e^{y\sqrt{ScKr}} \operatorname{erfc} \left(\frac{y\sqrt{Sc}}{2\sqrt{t}} + \sqrt{Kr t} \right) \right] \quad (5.30)$$

$$f_{10}(y, t) = \frac{e^{-a_7 t}}{2} \left[e^{-y\sqrt{Sc(Kr-a_7)}} \operatorname{erfc} \left(\frac{y\sqrt{Sc}}{2\sqrt{t}} - \sqrt{(Kr-a_7)t} \right) + e^{y\sqrt{Sc(Kr-a_7)}} \operatorname{erfc} \left(\frac{y\sqrt{Sc}}{2\sqrt{t}} + \sqrt{(Kr-a_7)t} \right) \right] \quad (5.31)$$

5.4.3 Nusselt Number

Expressions for Nusselt number Nu are deliberate from equations (5.9) and (5.12) using the relation

$$Nu = -\frac{v}{u_0(T-T_\infty)} \left(\frac{\partial T}{\partial y} \right)_{y=0} \quad (5.32)$$

For ramped wall temperature and ramped surface concentration:

$$Nu = -[h_6(t) - h_6(t-1)H(t-1)] \quad (5.33)$$

For isothermal temperature and ramped surface concentration:

$$Nu = -[h_5(t)] \quad (5.34)$$

5.4.4 Sherwood Number

Expression for Sherwood number Sh for Ramped temperature with ramped surface concentration is obtained from equation (5.10) using the relation

$$Sh = -\left(\frac{\partial C}{\partial y} \right)_{y=0} \quad (5.35)$$

For ramped wall temperature and ramped surface concentration:

$$Sh = -[h_9(t) - h_9(t-1)H(t-1)] \quad (5.36)$$

5.4.5 Skin Friction

Expressions for skin-friction are deliberate from Equations (5.11) and (5.13) using the relations

$$\tau^*(y, t) = -\mu\beta \left(1 + \frac{1}{\gamma} \right) \tau \quad (5.37)$$

$$\text{Where } \tau = \left. \frac{\partial u}{\partial y} \right|_{y=0} \quad (5.38)$$

For ramped wall temperature and ramped surface concentration:

$$\tau = h_{11}(t) + h_{18}(t) - h_{18}(t-1)H(t-1) \quad (5.39)$$

For isothermal temperature and ramped surface concentration:

$$\tau = h_{11}(t) + h_{15}(t) + h_{16}(t) - h_{16}(t-1)H(t-1) - h_{17}(t) - h_{14}(t) + h_{14}(t-1)H(t-1) \quad (5.40)$$

Where

$$h_{18}(t) = h_{12}(t) + h_{13}(t) + h_{14}(t) \quad (5.41)$$

$$h_{11}(t) = e^{a't} \sqrt{\frac{b+a'}{a}} \operatorname{erf}(\sqrt{(b+a')t}) - \frac{e^{-bt}}{\sqrt{\pi at}} \quad (5.42)$$

$$h_{12}(t) = a_{15}h_1(t) + a_{16}h_2(t) + a_{10}h_3(t) + a_{13}h_4(t) \quad (5.43)$$

$$h_{13}(t) = a_{11}h_5(t) + a_9h_6(t) + a_{10}h_7(t) \quad (5.44)$$

$$h_{14}(t) = a_{14}h_8(t) + a_{12}h_9(t) + a_{13}h_{10}(t) \quad (5.45)$$

$$h_{15}(t) = a_9h_1(t) - a_9h_3(t) \quad (5.46)$$

$$h_{16}(t) = a_{14}h_1(t) + a_{12}h_2(t) + a_{13}h_4(t) \quad (5.47)$$

$$h_{17}(t) = a_9h_5(t) - a_9h_7(t) \quad (5.48)$$

$$h_1(t) = -\sqrt{\frac{b}{a}} \operatorname{erf}(\sqrt{bt}) - \frac{e^{-bt}}{\sqrt{\pi at}} \quad (5.49)$$

$$h_2(t) = -\frac{1}{\sqrt{4ab}} \operatorname{erf}(\sqrt{bt}) - t \sqrt{\frac{b}{a}} \operatorname{erf}(\sqrt{bt}) - \frac{t e^{-bt}}{\sqrt{\pi at}} \quad (5.50)$$

$$h_3(t) = -e^{a_3 t} \sqrt{\frac{b+a_3}{a}} \operatorname{erf}(\sqrt{(b+a_3)t}) - \frac{e^{-bt}}{\sqrt{\pi at}} \quad (5.51)$$

$$h_4(t) = -e^{-a_7 t} \sqrt{\frac{b-a_7}{a}} \operatorname{erf}(\sqrt{(b-a_7)t}) - \frac{e^{-bt}}{\sqrt{\pi at}} \quad (5.52)$$

$$h_5(t) = -\sqrt{(-H) Pr} \operatorname{erf}(\sqrt{(-H)t}) - \sqrt{\frac{Pr}{\pi t}} e^{Ht} \quad (5.53)$$

$$h_6(t) = -\sqrt{\frac{Pr}{4(-H)}} \operatorname{erf}(\sqrt{(-H)t}) - t\sqrt{(-H) Pr} \operatorname{erf}(\sqrt{(-H)t}) - \sqrt{\frac{t Pr}{\pi}} e^{Ht} \quad (5.54)$$

$$h_7(t) = -e^{a_3 t} \sqrt{Pr(-H + a_3)} \operatorname{erf}(\sqrt{(-H + a_3)t}) - \sqrt{\frac{Pr}{\pi t}} e^{Ht} \quad (5.55)$$

$$h_8(t) = -\sqrt{Kr Sc} \operatorname{erf}(\sqrt{Krt}) - \sqrt{\frac{Sc}{\pi t}} e^{-Krt} \quad (5.56)$$

$$h_9(t) = -\sqrt{\frac{Sc}{4Kr}} \operatorname{erf}(\sqrt{Krt}) - t\sqrt{Sc Kr} \operatorname{erf}(\sqrt{Krt}) - \sqrt{\frac{t Sc}{\pi}} e^{-Krt} \quad (5.57)$$

$$h_{10}(t) = -e^{-a_7 t} \sqrt{Sc(Kr - a_7)} \operatorname{erf}(\sqrt{(Kr - a_7)t}) - \sqrt{\frac{Sc}{\pi t}} e^{-Krt} \quad (5.58)$$

$$h_{19}(t) = -\sqrt{Sc Kr} \operatorname{erf}(\sqrt{Krt}) - \sqrt{\frac{Sc}{\pi t}} e^{-Krt} \quad (5.59)$$

5.5 Results and Discussion

In order to get a clear insight of the physics of the problem, a parametric study is performed with the help of graphical illustrations. Expressions for the velocity, temperature and concentration profiles for several values of governing parameter are presented through Figures (5.2) to (5.11). Effect of Casson fluid parameter γ on velocity profiles is shown in Figure 5.2. It is found that velocity decreases with increase in γ . Figure 5.3 illustrates that the fluid velocity and boundary layer thickness decreases when M increases. Figure 5.4 illustrates effect of permeability of porous medium k on velocity profile. It is seen that, velocity increases with increase in k . Physically, with increase in k , size of holes increase, therefore motion of the fluid will be increased. Figure 5.2 to Figure 5.4 show strong agreement with previous published research work, which is done by Kataria and Patel [110]. Figure 5.5 and Figure 5.6 show effects of chemical reaction parameter Kr on velocity and concentration profiles for both thermal conditions. It is observed that buoyancy effects due to concentration are important in the channel. Moreover it is seen that velocity and concentration decrease with increase in chemical reaction parameter Kr . Physically, fluid becomes thicker due to increasing value of Kr which reduce concentration profiles.

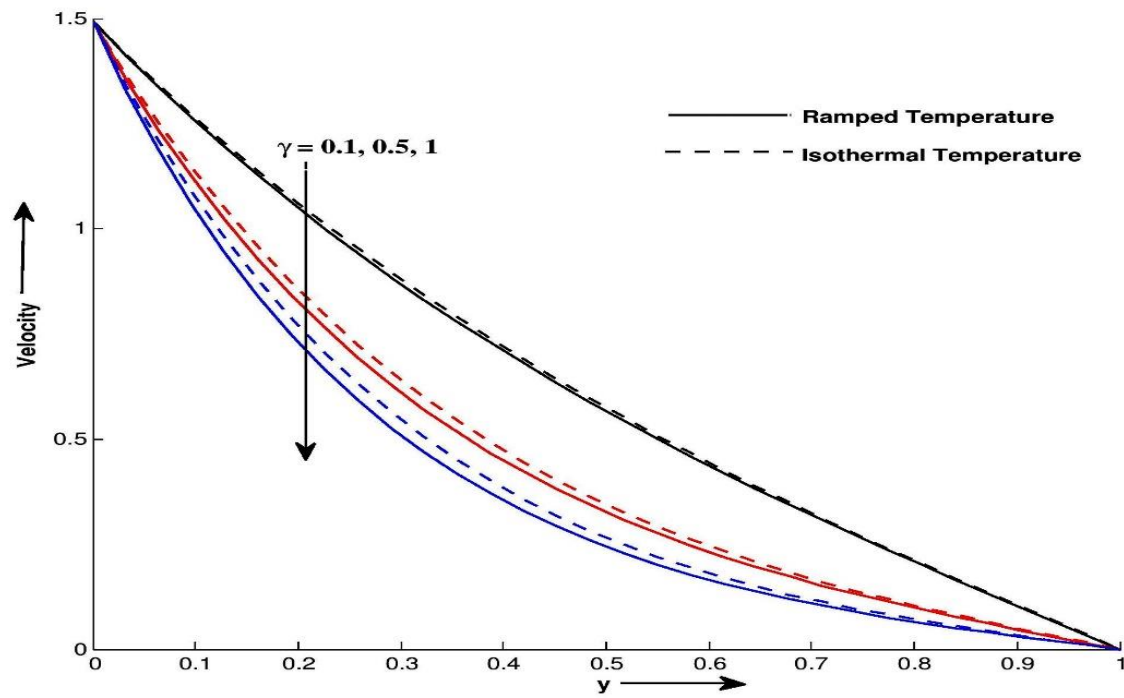


Figure 5.2: Velocity profile u for different values of y and γ at $Pr = 15, M = 5, k = 0.5, Sc = 0.66, Gm = 5, Gr = 10, Kr = 5, H = 2/3$ and $t = 0.4$

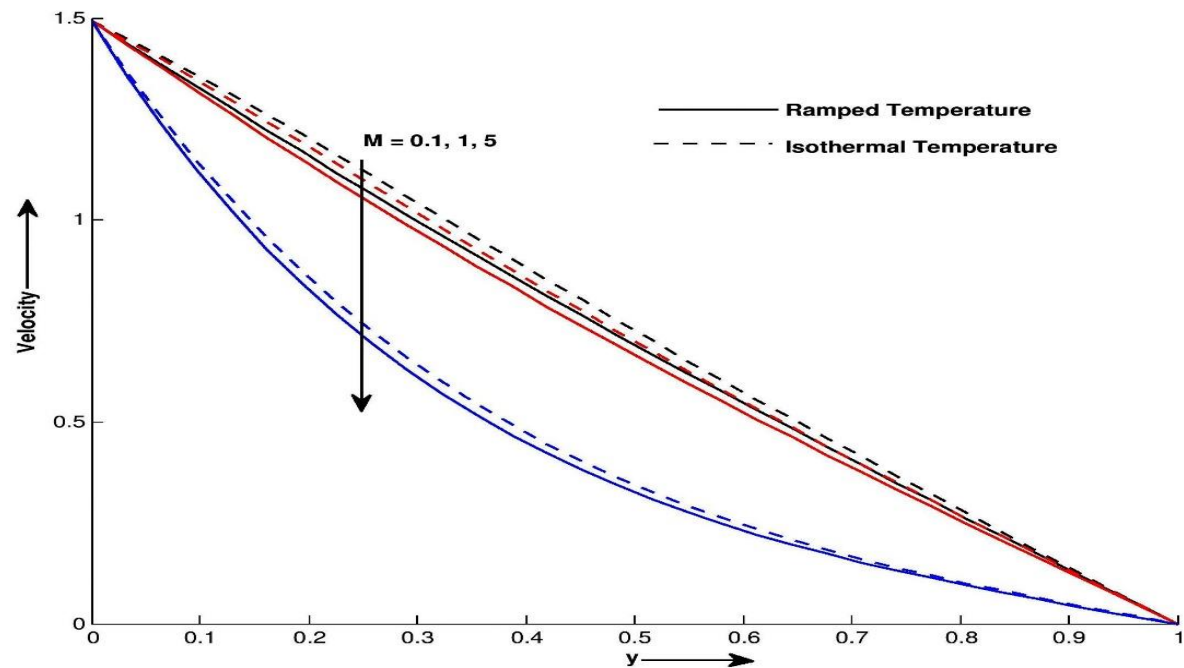


Figure 5.3: Velocity profile u for different values of y and M at $Pr = 15, \gamma = 0.5, k = 0.5, Sc = 0.66, Gm = 5, Gr = 10, Kr = 5, H = 2/3$ and $t = 0.4$

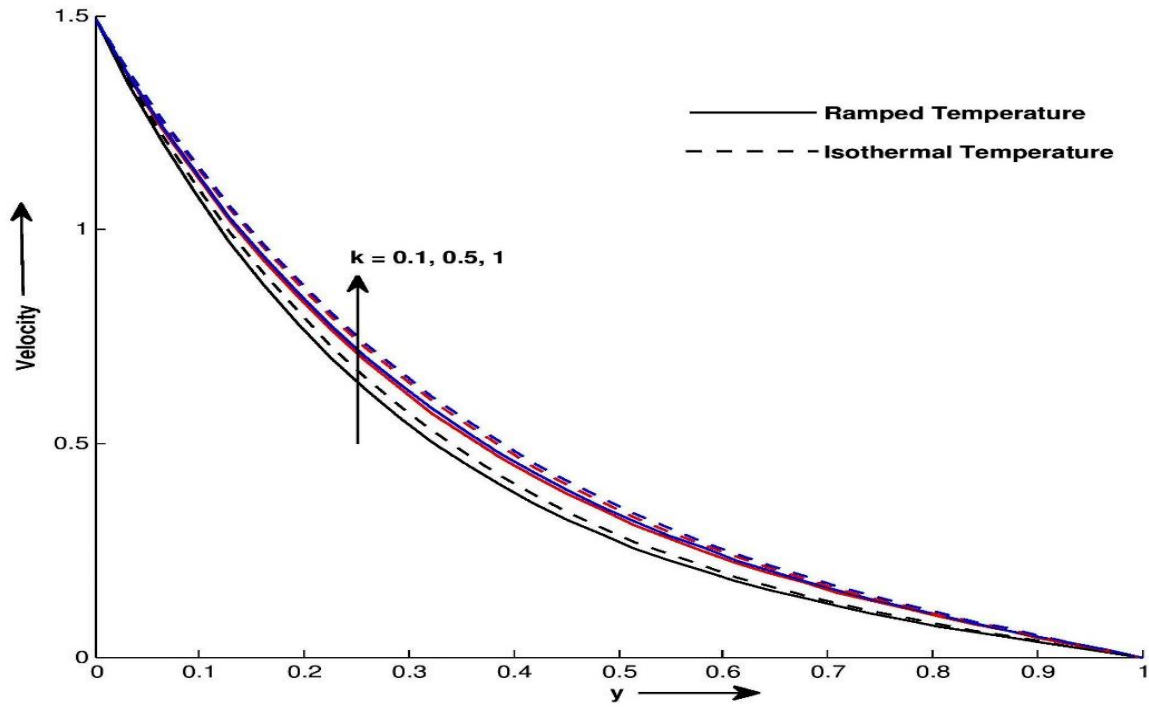


Figure 5.4: Velocity profile u for different values of y and k at $Pr = 15, \gamma = 0.5, M = 5, Sc = 0.66, Gm = 5, Gr = 10, Kr = 5, H = 2/3$ and $t = 0.4$

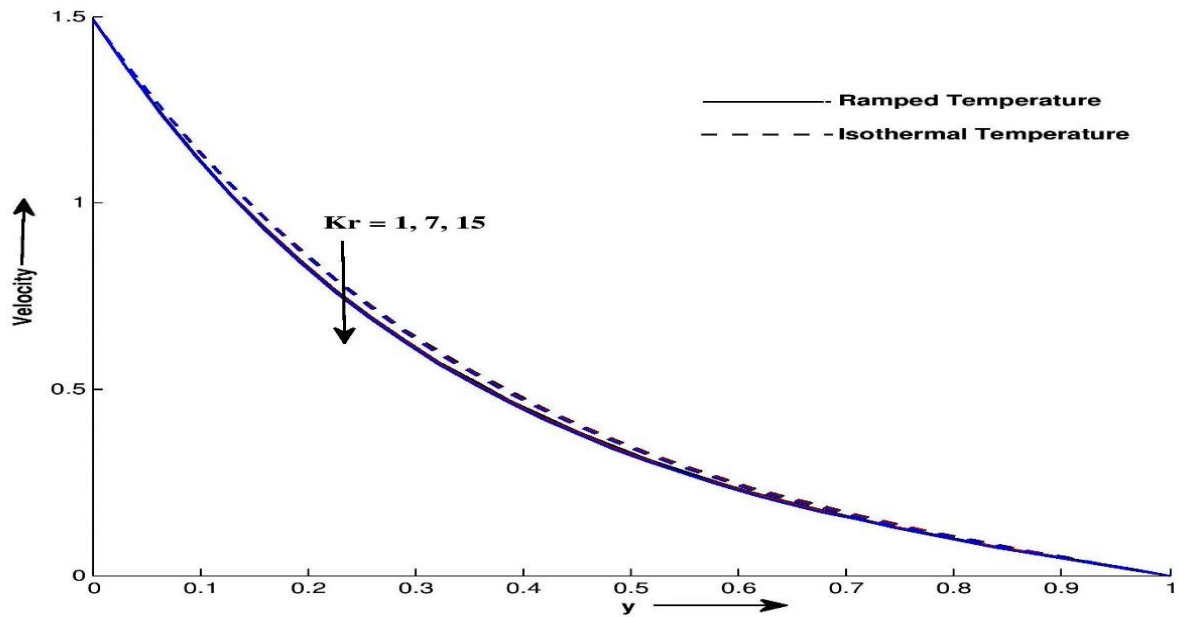


Figure 5.5: Velocity profile u for different values of y and Kr at $Pr = 15, \gamma = 0.5, M = 5, k = 0.5, Gm = 5, Sc = 0.66, Gr = 10, H = 2/3$ and $t = 0.4$

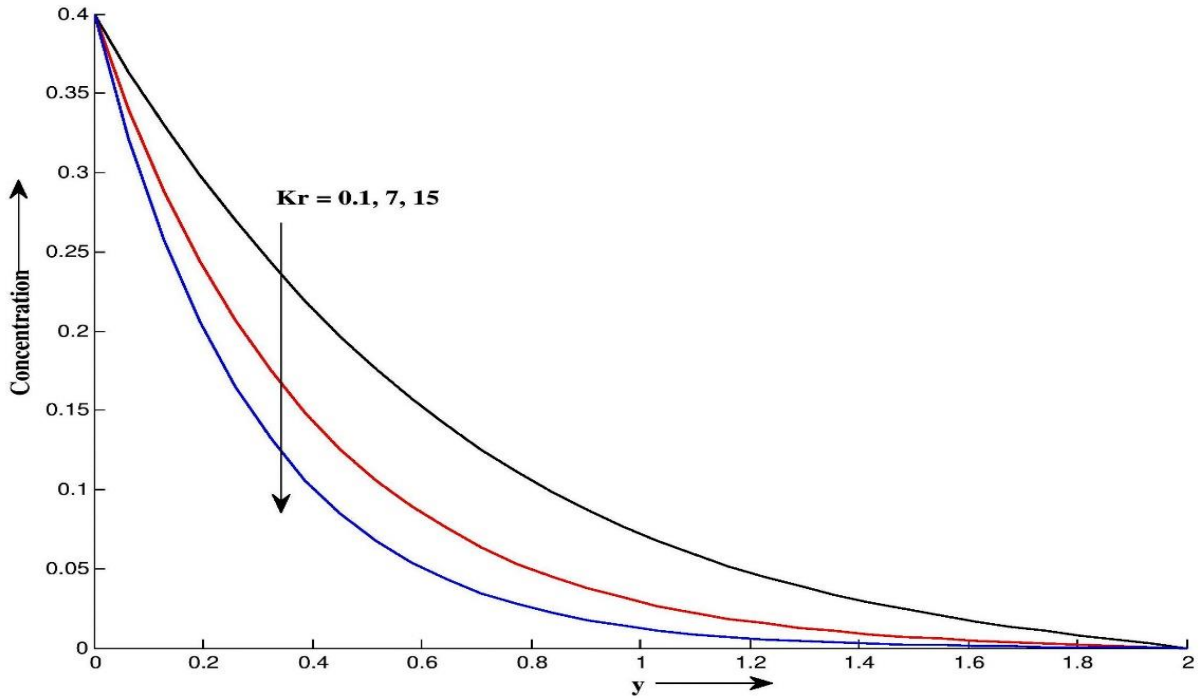


Figure 5.6: Concentration profile C for different values of y and Kr at $Sc = 0.66$ and $t = 0.4$

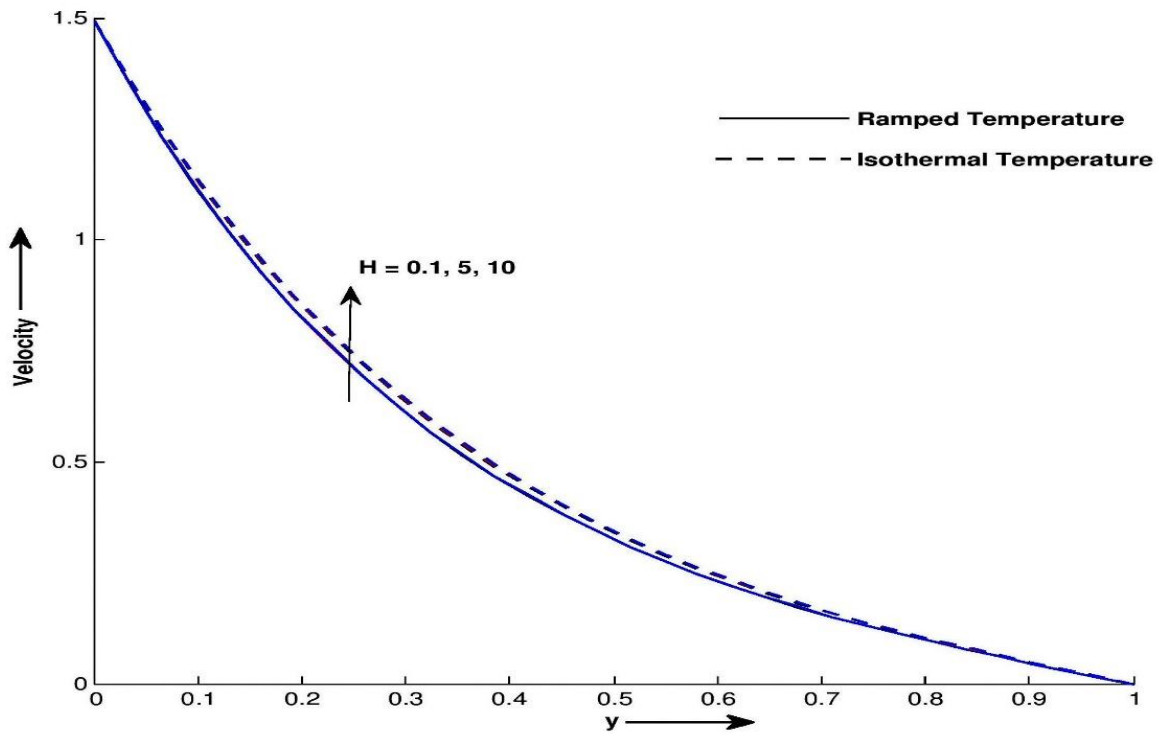


Figure 5.7: Velocity profile u for different values of y and H at $Pr = 15, \gamma = 0.5, M = 5, k = 0.5, Gm = 5, Sc = 0.66, Kr = 5, Gr = 10$ and $t = 0.4$

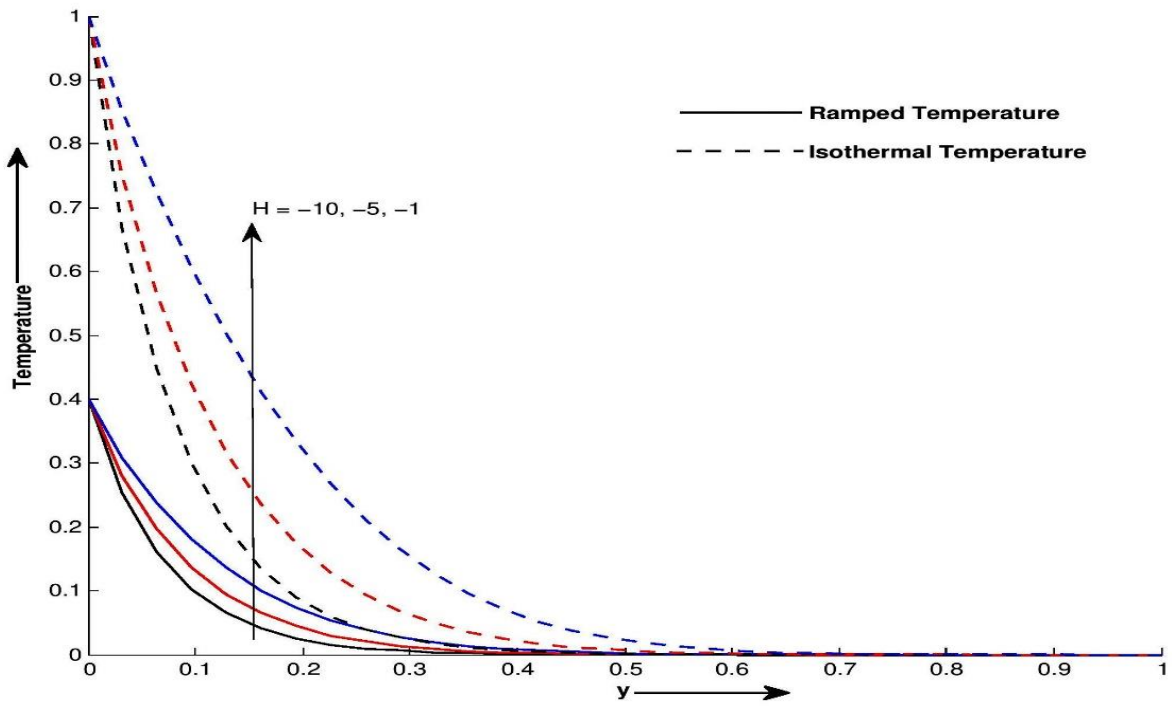


Figure 5.8: Temperature profile θ for different values of y and H at $Pr = 15$ and $t = 0.4$

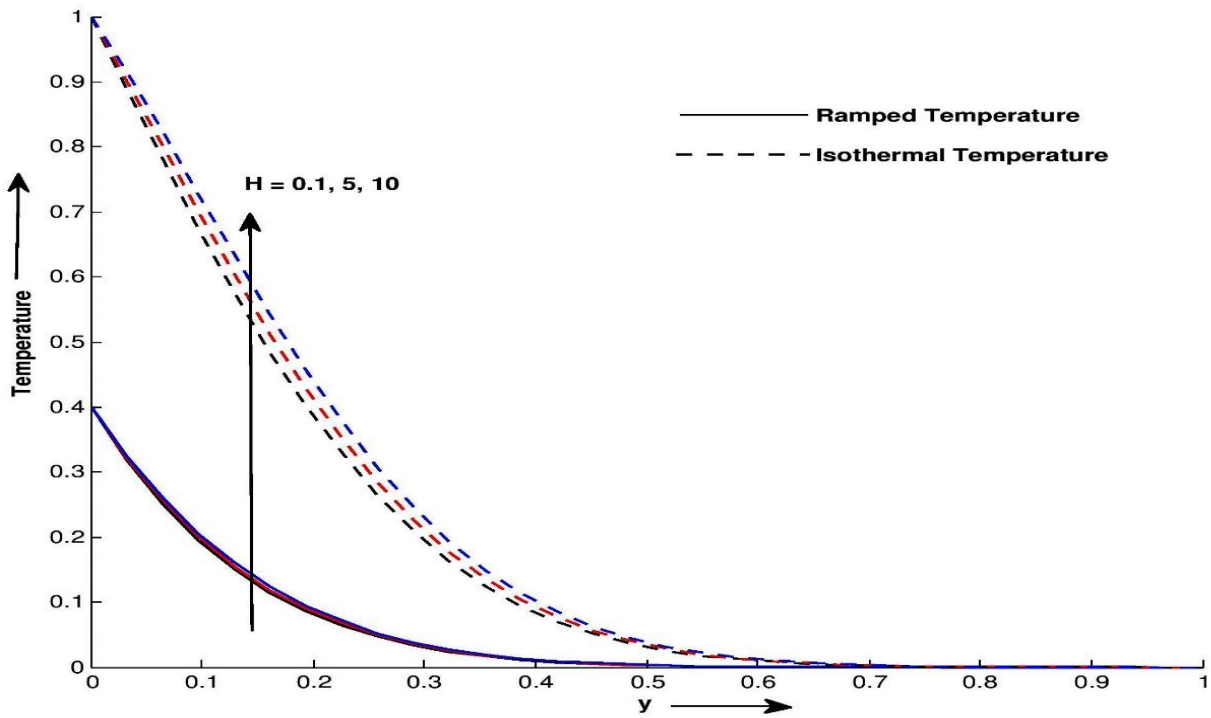


Figure 5.9: Temperature profile θ for different values of y and H at $Pr = 15$ and $t = 0.4$

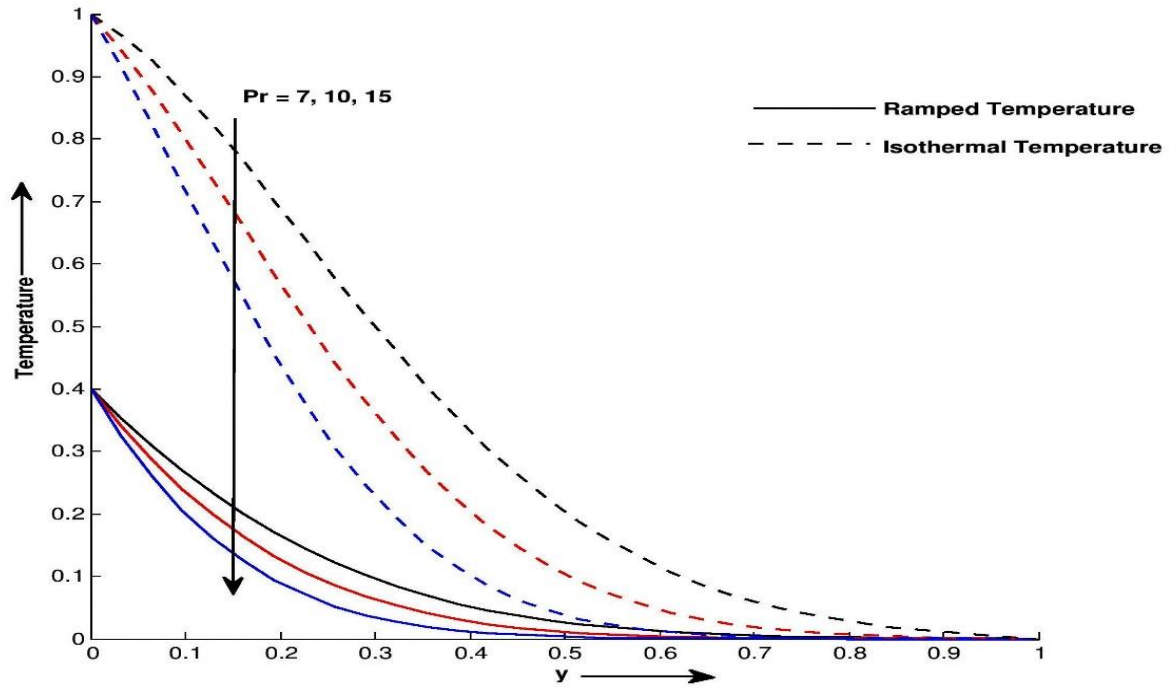


Figure 5.10: Temperature profile θ for different values of y and Pr at $H = 2/3$ and $t = 0.4$

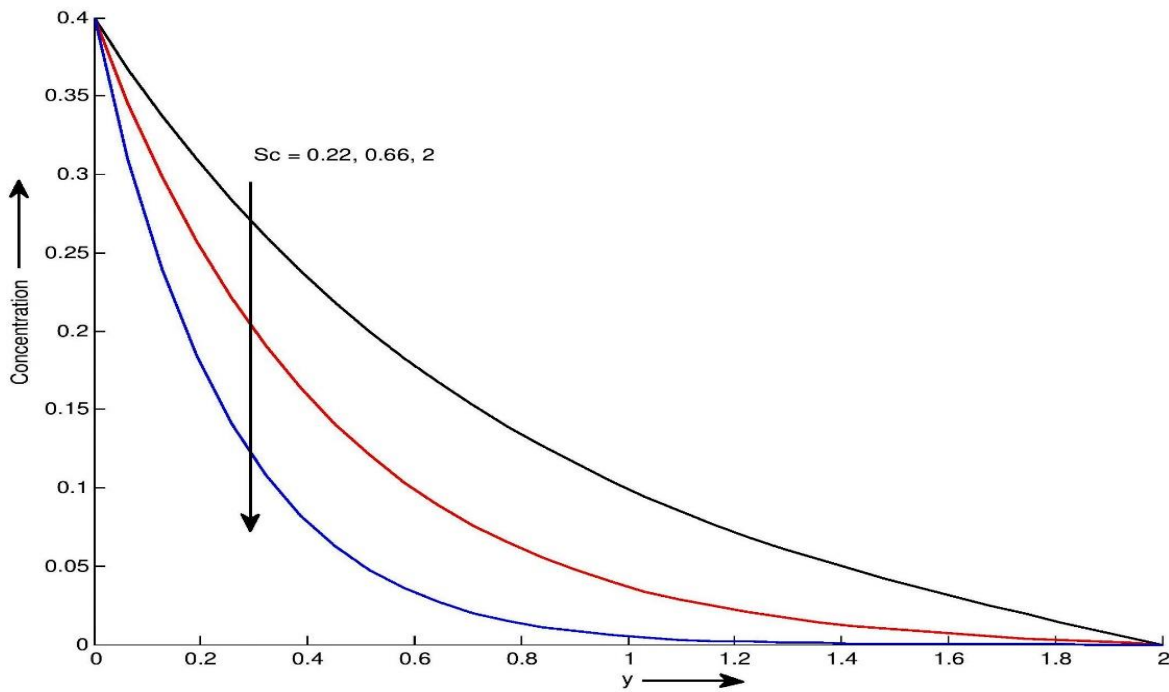


Figure 5.11: Concentration profile C for different values of y and Sc at $Kr = 5$ and $t = 0.4$

Figure 5.7 shows influence of heat generation H on velocity for both thermal conditions. It is seen that Heat source indicates generation of heat, which is improving the temperature in the flow field. Therefore, heat generation parameter tends to improve velocity profiles. Figure 5.8 and Figure 5.9 illustrate the effect of Heat absorption/heat generation H on temperature profile. The positive sign indicates the heat generation (heat source) whereas negative means heat absorption (heat sink). It is seen that heat source parameter H tends to increase temperature as well as motion of fluid flow. These results are clearly supported from the physical point of view. Figure 5.10 shows temperature of the fluid decreases with increase in Pr . In heat transfer problems, the Prandtl number controls thickness of the thermal boundary layers. When Pr is small, it means that the heat diffuses quickly. This means that for liquid metals, thickness of the temperature boundary layer is much bigger than the momentum boundary layer. The graphical results for Sc are shown in Figure 5.11. It is observed that the concentration decreases with increase in Sc . Physically, increase in Sc , kinematic viscosity rises which in turn reduces molecular diffusion, therefore concentration decreases.

Table 5.1: Skin friction variation

Pr	γ	Sc	Gr	Gm	Kr	M	k	H	t	Skin friction τ for Ramped temperature	Skin friction τ for isothermal temperature
15	0.5	0.66	3	4	5	2	0.8	-3	0.4	9.0249	5.7787
16	0.5	0.66	3	4	5	2	0.8	-3	0.4	9.0195	5.7880
17	0.5	0.66	3	4	5	2	0.8	-3	0.4	9.0147	5.7964
15	0.6	0.66	3	4	5	2	0.8	-3	0.4	9.0894	5.4333
15	0.7	0.66	3	4	5	2	0.8	-3	0.4	9.3156	5.1835
15	0.5	0.7	3	4	5	2	0.8	-3	0.4	8.7965	5.7809
15	0.5	0.8	3	4	5	2	0.8	-3	0.4	8.3953	5.7893
15	0.5	0.66	4	4	5	2	0.8	-3	0.4	9.0725	5.6669
15	0.5	0.66	5	4	5	2	0.8	-3	0.4	9.1201	5.5550
15	0.5	0.66	3	5	5	2	0.8	-3	0.4	9.6241	5.6860
15	0.5	0.66	3	6	5	2	0.8	-3	0.4	10.2233	5.5933
15	0.5	0.66	3	4	5.1	2	0.8	-3	0.4	8.9925	5.7686
15	0.5	0.66	3	4	5.2	2	0.8	-3	0.4	8.9588	5.7612
15	0.5	0.66	3	4	5	2.1	0.8	-3	0.4	9.3023	6.0465

15	0.5	0.66	3	4	5	2.2	0.8	-3	0.4	9.5520	6.3676
15	0.5	0.66	3	4	5	2	0.85	-3	0.4	8.9725	5.7331
15	0.5	0.66	3	4	5	2	0.9	-3	0.4	8.9255	5.6930
15	0.5	0.66	3	4	5	2	0.8	-2	0.4	9.0331	5.7429
15	0.5	0.66	3	4	5	2	0.8	-1	0.4	9.0144	5.6809
15	0.5	0.66	3	4	5	2	0.8	-3	0.5	10.5195	6.3008
15	0.5	0.66	3	4	5	2	0.8	-3	0.6	12.1087	6.9069

Table 5.2: Nusselt number variation

Pr	H	t	Nusselt number Nu for Ramped Temperature	Nusselt number Nu for isothermal Temperature
15	-3	0.4	3.7563	6.9349
16	-3	0.4	3.8795	7.1623
17	-3	0.4	3.9989	7.3827
15	-2	0.4	3.4481	5.9019
15	-1	0.4	3.1185	4.7517
15	-3	0.5	4.4445	6.8392
15	-3	0.6	5.1256	6.7869

Table 5.3: Sherwood Number variation

Kr	Sc	t	Sherwood Number for Ramped wall concentration Sh	Sherwood Number for constant concentration Sh
5	0.66	0.4	0.9062	1.8320
5.1	0.66	0.4	0.9118	1.8493
5.2	0.66	0.4	0.9173	1.8664
5	0.7	0.4	0.9333	1.8867
5	0.8	0.4	0.9977	2.0170
5	0.66	0.5	1.0889	1.8238
5	0.66	0.6	1.2711	1.8201

Table 5.4: Velocity, Temperature and Concentration profile for ramped wall temperature of different step size at $M = 0.5, k = 0.5, Pr = 15, Sc = 0.66, Gm = 5, Gr = 10, H = 10, Kr = 5$ and $\gamma = 0.5$

y	u for Step size 31 & 6 of y and t on [0 1]	u for Step size 101 & 51 of y and t on [0 1]	θ for Step size 31 & 6 of y and t on [0 1]	θ for Step size 101 & 51 of y and t on [0 1]	C for Step size 31 & 6 of y and t on [0 1]	C for Step size 101 & 51 of y and t on [0 1]
0.2	0.8268	0.8268	0.0894	0.0894	0.2502	0.2502
0.4	0.4488	0.4488	0.0118	0.0118	0.1521	0.1521
0.6	0.2317	0.2317	0.0009	0.0009	0.0861	0.0861
0.8	0.0982	0.0982	0.0000	0.0000	0.0388	0.0388

Table 5.5: Velocity, Temperature and Concentration profile for isothermal temperature of different step size at $M = 0.5, k = 0.5, Pr = 15, Sc = 0.66, Gm = 5, Gr = 10, H = 10, k = 5$ and $\gamma = 0.5$

y	u for Step size 31 & 6 of y and t on [0 1]	u for Step size 101 & 51 of y and t on [0 1]	θ for Step size 31 & 6 of y and t on [0 1]	θ for Step size 101 & 51 of y and t on [0 1]	C for Step size 31 & 6 of y and t on [0 1]	C for Step size 101 & 51 of y and t on [0 1]
0.2	0.8575	0.8575	0.4404	0.4404	0.2502	0.2502
0.4	0.4734	0.4734	0.1016	0.1016	0.1521	0.1521
0.6	0.2452	0.2452	0.0122	0.0122	0.0861	0.0861
0.8	0.1038	0.1038	0.0008	0.0008	0.0388	0.0388

Table 5.6: Comparison of Nusselt number with Ref. [151] and Ref. [150]

t	-H	Pr	Nu for ramped temp. Ref [151]	Nu for ramped temp. Ref [150]	Nu for rampe d temp.	Nu for isothermal temp. Ref [151]	Nu for isotherma l temp. Ref [150]	Nu for isother mal temp.
0.3	1	0.71	0.57134752	0.571348	0.5713	1.11605411	1.11605	1.1161
0.5	1	0.71	0.77913255	0.779133	0.7791	0.98302070	0.983021	0.9830
0.7	1	0.71	0.96929143	0.969291	0.9693	0.92531051	0.925311	0.9253
0.7	1	0.71	0.96929143	0.969291	0.9693	0.92531051	0.925311	0.9253

0.7	3	0.71	1.26243402	1.26243	1.2624	1.47003548	1.47004	1.4700
0.7	5	0.71	1.50704023	1.50704	1.5070	1.88594507	1.88595	1.8859
0.7	1	0.50	0.81341130	-	0.8134	0.77650333	-	0.7765
0.7	1	0.71	0.96929143	-	0.9693	0.92531051	-	0.9253
0.7	1	7.00	3.04350641	-	3.0435	2.90540943	-	2.9054

Table 5.1 shows skin friction variant for different physical parameters. For both thermal conditions, Kr , k and H tend to reduce skin friction whereas M and t have reverse effects on it. From Table 5.2, it is observed that Pr tends to improve Nusselt number whereas heat absorption H has reverse effect on it. From Table 5.3, it is seen that Sherwood number increase tendency with Kr and Sc . The governing partial differential equations 5.5 to 5.8 with initial and boundary conditions 5.10 are solved numerically using Matlab software. In entire numerical computations, increment step along t is 0.2 and y is 0.0323. This attentive problem requests the solution on mesh produced by spaced points from the spatial interval 32 values of y from the space interval $[0, 1]$ and 6 values of t from the time interval $[0, 1]$. Table 5.4 and Table 5.5 verify that solution of velocity, temperature and concentration profile are independent of step size for all thermal and concentration boundary conditions. Table 5.6 demonstrate that Nusselt number and Sherwood number for both thermal conditions strong agreement with Nandkeolyar et al. [151] and Seth et al. [150].

5.6 Concluding Remark

Main Significant outcomes of the study are as follows:

- Permeability of porous medium k and heat generation/absorption H tends to improve fluid velocity whereas Magnetic parameter M , Casson parameter γ and chemical reaction Kr have reverse effect on it.
- Temperature decreases tendency with Pr whereas increase tendency with H .
- Concentration decreases tendency with Schmidt number Sc and chemical reaction parameter Kr .
- Skin friction rises while Nusselt number falls with increase in Pr .
- Sherwood number rises with increase in Kr , Sc and t .